Journal of Pharmacological and Toxicological Methods 127 (2024) 107516

Contents lists available at ScienceDirect

Journal of Pharmacological and Toxicological Methods

journal homepage: www.elsevier.com/locate/jpharmtox

Research article

A genetic algorithm-based approach for the prediction of metabolic drug-drug interactions involving CYP2C8 or CYP2B6

Veronica Di Paolo [a,*], Francesco Maria Ferrari [b], Davide Veronese [a], Italo Poggesi [c], Luigi Quintieri [a,*]

[a] Laboratory of Drug Metabolism, Department of Pharmaceutical and Pharmacological Sciences, University of Padova, Padova, Italy
[b] Department R&D, MeteRSit, Padova, Italy
[c] Clinical Pharmacology, Modeling and Simulation, GlaxoSmithKline S.p.A., Verona, Italy

ARTICLE INFO

Keywords:
Drug-drug interactions
Cytochrome P450
Clinical pharmacokinetics
Genetic algorithm

ABSTRACT

Background and objectives: A genetic algorithm (GA) approach was developed to predict drug-drug interactions (DDIs) caused by cytochrome P450 2C8 (CYP2C8) inhibition or cytochrome P450 2B6 (CYP2B6) inhibition or induction. Nighty-eight DDIs, obtained from published in vivo studies in healthy volunteers, have been considered using the area under the plasma drug concentration–time curve (AUC) ratios (i.e., ratios of AUC of the drug substrate administered in combination with a DDI perpetrator to AUC of the drug substrate administered alone) to describe the extent of DDI.

Methods: The following parameters were estimated in this approach: the contribution ratios (CR_{CYP2B6} and CR_{CYP2C8}, i.e., the fraction of the dose metabolized via CYP2B6 or CYP2C8, respectively) and the inhibitory or inducing potency of the perpetrator drug (IR_{CYP2B6}, IR_{CYP2C8} and IC_{CYP2B6}, for inhibition of CYP2B6 and CYP2C8, and induction of CYP2B6, respectively). The workflow consisted of three main phases. First, the initial estimates of the parameters were estimated through GA. Then, the model was validated using an external validation. Finally, the parameter values were refined via a Bayesian orthogonal regression using all data.

Results: The AUC ratios of 5 substrates, 11 inhibitors and 19 inducers of CYP2B6, and the AUC ratios of 19 substrates and 23 inhibitors of CYP2C8 were successfully predicted by the developed methodology within 50–200% of observed values.

Conclusions: The approach proposed in this work may represent a useful tool for evaluating the suitable doses of a CYP2C8 or CYP2B6 substrates co-administered with perpetrators.

1. Introduction

Simultaneous administration of multiple drugs is particularly common in elderly subjects, exposing them to a potential risk of drug-drug interactions (DDIs). Furthermore, a per capita increase in drug intake has been observed in recent years. According to data from Centers for Disease Control, between 1988 and 2010, the percentage of American people taking three or more prescribed drugs doubled, while the percentage of subjects taking five or more drugs nearly tripled (Percha & Altman, 2013). The occurrence of DDIs represents a clinically relevant problem which positively correlates with the number of co-administered drugs. DDIs may compromise therapeutic success, or even be the cause of serious health complications requiring hospitalization (Ferdousi et al., 2017). Moreover, errors in multiple drug prescriptions may lead to DDIs causing high costs related to diagnosis and patient treatment, as well as health risks for the patients.

Different DDI predictive approaches based on the generation of in vitro data or on the examination of data available in the literature have been proposed (Yoshida et al., 2017). These approaches may have been combined with chemo-informatics methodologies (Ferdousi et al., 2017; Percha & Altman, 2013). For instance, integration of the available structural, in vitro and in vivo data using physiology-based pharmacokinetics models (PBPK) using standard platforms, as SIMCYP, has become more and more popular (see, e.g., Abouir et al., 2021; Sinha et al., 2012). Nowadays, as it is the case of many other applications in the field of drug development, the focus is shifting on the prediction of potential DDIs through computational methods based on artificial intelligence and machine learning approaches (Ferreira & Andricopulo,

* Corresponding authors at: Department of Pharmaceutical and Pharmacological Sciences, Largo Egidio Meneghetti, 2 I-35131, Padova, Italy.
E-mail addresses: veronica.dipaolo@unipd.it (V. Di Paolo), luigi.quintieri@unipd.it (L. Quintieri).

https://doi.org/10.1016/j.vascn.2024.107516
Received 29 March 2024; Received in revised form 14 May 2024; Accepted 16 May 2024
Available online 20 May 2024

2019; Gaurav et al., 2021). Unlike in vitro and in vivo studies which are time-consuming and expensive, computational approaches allow an easier and quicker collection and manipulation of large amounts of data (Han et al., 2022). In this perspective, we developed a genetic algorithm (GA)-based approach, built on the framework proposed by Ohno and collaborators (Ohno et al., 2007), to predict DDIs caused by inhibition of cytochrome P450 2C8 (CYP2C8) or inhibition or induction of cytochrome P450 2B6 (CYP2B6). Both CYP2C8 and CYP2B6 are enzymes well known to be involved in the clearance of many therapeutic agents in human, and to be induced or inhibited by several drugs, resulting in DDIs of clinical relevance (Backman et al., 2016; Quintieri et al., 2011; Wang & Tompkins, 2008).

GAs represent artificial intelligence tools that mimic the processes of biological natural selection and are successfully used as search algorithms to describe phenomena that do not have their own physical law or a priori knowledge, but are based only on observed data (Schmidt & Lipson, 2009). A basic GA consists of an initial finite number of individuals (population), representing possible solutions of the problem that "evolve" from generation to generation guaranteeing optimized solutions (Dong & Peng, 2011). The initial population should be large and sufficiently variable. After an initial evaluation, the GA proceeds with the selection of the individuals representing the best solutions in terms of fitness function. These individuals are then modified via crossover (a process that combines two solutions) or mutation (a process that incorporate a small random change), an approach that incorporates both stochastic and deterministic processes. Therefore, two aspects are combined together in the GA: the rules of survival of the fittest individuals in the process of biological evolution and random component of information exchange among the individuals of the population (Kramer, 2017). The measure of "goodness" (quality of solutions) of this computational model is called "fitness", analogous to the concept of "fitness" used in population ecology to indicate how well an organism adapts to its environment (Kramer, 2017; Sale & Sherer, 2015). The fitness function is phenomenon-specific and directly affects the convergence speed and the search for an optimized solution (Kramer, 2017).

In this work a fitness function was adopted to predict the extent of CYP2B6 and CYP2C8 inhibition-based DDIs, as well as CYP2B6 induction-based DDIs, expressed as area under the plasma drug concentration–time curve (AUC) ratios (i.e., ratios of AUC of the substrate administered in combination with a DDI perpetrator to AUC of the drug substrate administered alone).

2. Materials and methods

In this study we adopted a framework similar to that initially developed by Ohno et al. (Ohno et al., 2007), and that we have earlier used for the prediction of pharmacokinetic-based DDIs elicited by inhibition of CYP2C8 (Di Paolo et al., 2021) or by inhibition or induction of CYP2B6 (Di Paolo et al., 2022). For DDIs caused by CYP2C8 or CYP2B6 inhibition, the AUC ratio is calculated from Equation (Eq. (1)).

$$\frac{AUC^*}{AUC} = \frac{1}{1 - CR^*IR} \quad (1)$$

where AUC is the AUC of the CYP2B6 or CYP2C8 substrate drug when administered alone; AUC* is the AUC of the substrate drug when co-administered with a CYP2B6 or a CYP2C8 inhibitor. CR_{CYP2B6} and CR_{CYP2C8} are the contribution ratios (i.e., the fractions of the substrate's oral clearance due to metabolism via CYP2B6 and CYP2C8, respectively). AUC values were obtained from the open literature (see Section 2.1, values were typically calculated using standard non-compartmental analysis). CRs are positive numbers between 0 (no contribution of the specific metabolic route) and 1 (the compound is entirely metabolized via the specific metabolic route). IR_{CYP2B6} and IR_{CYP2C8} are the inhibition ratios for the inhibitor. IR represents the in vivo potency of the inhibitor integrated over time and is related to both the dose (and thus exposure) of the inhibitor and its inhibition constant (K_i). IR values are also positive numbers between 0 (no inhibitory effect towards the specified enzyme) and 1 (the inhibitor is able to completely wipe the activity of the specified enzyme). Based on this, the AUC ratios (AUCR; AUC*/AUC) for inhibition are positive real numbers between 1 (no inhibitory effect; AUC with the inhibitor is equal to the AUC without inhibitor) and infinite (complete inhibition of the elimination; the substrate, when eliminated solely by the specified enzyme, cannot be eliminated from the body).

For DDIs caused by induction of CYP2B6, the AUC ratio is calculated from Eq. (2).

$$\frac{AUC^*}{AUC} = \frac{1}{1 + CR^*IC} \quad (2)$$

where, similarly to inhibition, AUC is the AUC of the substrate drug when it is orally administered alone; AUC* is the AUC of the substrate drug when it is co-administered with a CYP2B6 inducer. CR_{CYP2B6} is the contribution ratio, defined as previously described regarding inhibition. IC_{CYP2B6} is the apparent increase in clearance of substrates caused by induction of CYP2B6. IC_{CYP2B6} quantifies the inducer potency in a range from 0 to any positive value and, as $IR_{CYP2B6/CYP2C8}$, depends on both the dose and the potency of the inducer and, in this case, also the duration of the treatment with the inducer (Ohno et al., 2008). Details on the rationale and demonstration of the equations are available in the work of Ohno et al. (Ohno et al., 2007; Ohno et al., 2008).

This approach was implemented using a GA-based computational methodology. The approach consisted of 3 steps for each of the two enzymes: (1) initial estimation of model parameters (CR_{CYP2B6}, CR_{CYP2C8}, IR_{CYP2B6}, IR_{CYP2C8} and IC_{CYP2B6} values) through GA; (2) external validation of predicted values; and (3) final estimation of the parameter values using all data.

2.1. Step 1: initial estimation of parameters through GA

For the evaluation of DDIs mediated by CYP2B6 or CYP2C8 inhibition, AUCR reported in the Resources of the Drug Interaction Database of the University of Washington [http://www.druginteractioninfo.org] were used. Moreover, data published in peer-review journals were also considered. AUC values used in our computational model are reported in Tables 1 and 2.

Unlike in the study by Ohno et al. (Ohno et al., 2007), in which a CR or IR value was assumed a priori and, subsequently, CRs and IRs were calculated according to a trial-and-error approach with manual calculation, our GA-based computational method was initialized with random CRs, IRs and ICs values. GAs mimic the natural selection process in evolution to solve the global optimization problem (Holland, 1992). To limit the space of possible values and drive the GA, the only constraints used were based on the definition of the parameters and are represented in Figs. 1 and 2, which are plots of Eqs. (1) and (2), respectively (MATLAB software, version R2013b, MathWorks Inc., Natick, MA, USA). In particular, Fig. 1 shows the possible values of CR_{CYP2B6}, CR_{CYP2C8}, IR_{CYP2B6} and IR_{CYP2C8} for a fixed AUCR. It is noteworthy that, for high values of AUCR, the possible values of CR_{CYP2B6}, CR_{CYP2C8}, IR_{CYP2B6} and IR_{CYP2C8} were more restricted than for lower AUC values. In the case of the perpetrator-victim couple gemfibrozil-dasabuvir, the AUCR value was 11.3 (see Table 1), and the possible values of IR_{CYP2B6}, IR_{CYP2C8}, CR_{CYP2B6} and CR_{CYP2C8} were between 0.9 and 0.99 (Fig. 1). Fig. 2 displays the possible values of AUCR based on CR_{CYP2B6} and IC_{CYP2B6} values. The upper limit value for IC_{CYP2B6} was 10, while the lower one was 0.2. The GA was guided by the constraints of Fig. 1 for the prediction of DDIs elicited by enzyme inhibition, whereas the constraints of Fig. 2 were considered for DDIs caused by enzyme induction. The set constraints limit the upper and lower boundaries for the individuals of new populations. For predictions by GA of DDIs caused by

Table 1
Drug-Drug interaction studies used for predicting the interactions mediated by CYP2C8 inhibition.

Inhibitor (dose)	Substrate	Step	Observed AUC ratio	Reference
Gemfibrozi (600 mg BID x 5 days)	Daprodustat	*Step 1*	17.36	Johnson et al., 2014
Gemfibrozil (600 mg BID x 5 days)	Dasabuvir	*Step 1*	11.30	Menon et al., 2015
Gemfibrozil (900 mg SD)	Repaglinide	*Step 2*	8.26	Honkalammi et al., 2011
Gemfibrozil (600 mg BID x 3 days)	Cerivastatin (acid)	*Step 1*	5.60	Backman et al., 2002
Gemfibrozil (600 mg BID x 4 days)	Pioglitazone	*Step2*	4.66	Aquilante et al., 2013
Gemfibrozil (600 mg BID x 3 days)	Enzalutamide	*Step 1*	4.04	Gibbons et al., 2015
Gemfibrozil (600 mg BID x 3 days)	Montelukast	*Step 2*	4.54	Karonen et al., 2010
Gemfibrozil (600 mg BID x 3 days)	Cerivastatin (lactone)	*Step 2*	4.40	Backman et al., 2002
Gemfibrozil (600 mg BID x 3 days)	Sinvastatin (acid)	*Step 1*	2.90	Backman et al., 2000
Gemfibrozil (600 mg BID x 3 days)	Rosiglitazone	*Step 2*	2.30	Niemi et al., 2003
Gemfibrozil (600 mg BID x 3 days)	Loperamide	*Step 1*	2.20	Niemi et al., 2006
Gemfibrozil (600 mg BID x 3 days)	Treprostinil	*Step 1*	1.90	FDA, 2009
Gemfibrozil (600 mg BID x 3 days)	Dabrafenib	*Step 1*	1.50	Suttle et al., 2015
Gemfibrozil (600 mg BID x 3 days)	Sitagliptin	*Step 2*	1.50	Arun et al., 2012
Gemfibrozil (600 mg BID x 3 days)	Ezetimibe	*Step 1*	1.40	Reyderman et al., 2004
Gemfibrozil (600 mg BID x 3 days)	Paritaprevir	*Step 2*	1.40	Menon et al., 2015
Gemfibrozil (600 mg BID x 3 days)	Simvastatin (lactone)	*Step 2*	1.40	Backman et al., 2000
Gemfibrozil (600 mg BID x 3 days)	R-Ibuprofen	*Step 1*	1.30	Tornio et al., 2007
Clopidrogrel (300 mg SD)	Repaglinide	*Step 1*	5.08	Tornio et al., 2014
Clopidrogrel (300 mg then 75 mg QD x 3 days)	Dasabuvir	*Step 1*	4.66	Itkonen et al., 2019
Clopidrogrel (300 mg then 75 mg QD x 3 days)	Pioglitazone	*Step 1*	2.15	Itkonen et al., 2016
Clopidrogrel (300 mg then 75 mg QD x 2 days)	Montelukast	*Step 1*	1.98	Itkonen et al., 2018
Letermovir (480 mg QD x 10 days)	Repaglinide	*Step 1*	2.47 (PBPK)	FDA, 2017
Letermovir (480 mg QD x 10 days)	Rosiglitazone	*Step 1*	1.46 (PBPK)	FDA, 2017
Teriflunomide (14–70 mg QD x 12 days)	Repaglinide	*Step 1*	2.42	FDA, 2012
Deferasirox (30 mg/kg QD x 3 days)	Repaglinide	*Step 1*	2.27	Skerjanec et al., 2010
Trimethoprim (200 mg SD)	Repaglinide	*Step 2*	1.82	Kim et al., 2016
Trimethoprim (960 mg BID x 6 days)	Amodiaquine	*Step 1*	1.60	Akande et al., 2015
Trimethoprim (160 mg BID x 6 days)	Pioglitazone	*Step 1*	1.55	Tornio et al., 2008
Trimethoprim (160 mg BID x 3 days)	Cerivastatin (lactone)	*Step 2*	1.50	Backman et al., 2003
Trimethoprim (160 mg BID x 3 days)	Cerivastatin (acid)	*Step 2*	1.40	Backman et al., 2003
Trimethoprim (160 mg BID x 4 days)	Rosiglitazone	*Step 2*	1.37	Niemi et al., 2004
Tazemetostat (800 mg BID at steady state)	Repaglinide	*Step 1*	1.80	FDA, 2019a
Efavirenz (400 mg daily x 12 days)	Amodiaquine	*Step 1*	1.80	Soyinka et al., 2013
Telithromycin (800 mg QD x 3 days)	Repaglinide	*Step 2*	1.77	Kajosaari et al., 2006
Tucatinib (300 mg BID x 10 days)	Repaglinide	*Step 1*	1.70	FDA, 2019a
Duvelisib (25 mg BID x 6 days)	Repaglinide	*Step 1*	1.54 (PBPK)	FDA, 2018a
Fedratinib (400 mg QD x 15 days)	Repaglinide	*Step 1*	1.46 (PBPK)	FDA, 2020a
Ketoconazole (200 mg BID x 5 days)	Rosiglitazone	*Step 1*	1.46	Park et al., 2004
Ketoconazole (400 mg QD x 6 days)	Dasabuvir	*Step 2*	1.42	FDA, 2014
Abiraterone acetate (1000 mg SD)	Pioglitazone	*Step 1*	1.42	Monbaliu et al., 2016
Atazanavir (400 mg QD x 6 days)	Rosiglitazone	*Step 1*	1.40	FDA, 2015a
Cotrimoxazole (160/800 mg BID x 6 days)*	Dasabuvir	*Step 1*	1.33	Polepally et al., 2016
Irbesartan (300 mg QD x 5 days)	Repaglinide	*Step 2*	1.33	Pei et al., 2018
Capmatinib (400 mg BID x 10 days)	Repaglinide	*Step 2*	1.32	FDA, 2020b
Lesinurad (400 mg SD)	Repaglinide	*Step 1*	1.31	FDA, 2015b
Tecovirimat (600 mg BID x 15 days)	Repaglinide	*Step 2*	1.29	FDA, 2018b
Amodiaquine (600 mg SD)	Pioglitazone	*Step 1*	1.28	Edema et al., 2018
Rolapitant (200 mg SD)	Repaglinide	*Step 1*	1.27	FDA, 2015c
Fluvoxamine (50 mg BID x 3.5 days)	Rosiglitazone	*Step 1*	1.25	Pedersen et al., 2006

BID: twice daily; PBPK: values obtained via physiology-based pharmacokinetic modeling; QD: once daily; SD: single dose; *Step 1*: values used in the initial estimation of CRs and IRs; *Step 2*: values used in the external validation. Unless otherwise specified, the administration route is oral.

* Cotrimoxazole: combination of trimethoprim and sulfamethoxazole.

CYP2C8 inhibition, 33 $AUCR_{CYP2C8}$, 15 CR_{CYP2C8} and 19 IR_{CYP2C8} values were considered, while for DDIs elicited by CYP2B6 inhibition or induction, 32 $AUCR_{CYP2B6}$, 5 CR_{CYP2B6}, 10 IR_{CYP2B6} and 19 IC_{CYP2B6} values were considered.

Each individual is composed by the vector of the values of CR_{CYP2C8} and IR_{CYP2C8}: [CR_{C1}, CR_{C2}, …, CR_{C15}, IR_{C1}, IR_{C2}, … IR_{C19},] (CYP2C8 inhibition) or by the vector of the values of CR_{CYP2B6}, IR_{CYP2B6} and IC_{CYP2B6}: [CR_{B1}, CR_{B2}, …, CR_{B5}, IR_{B1}, IR_{B2}, … IR_{B10}, IC_{B1}, IC_{B2}, …IC_{B19}] (CYP2B6 inhibition or induction) which collectively represents the vectors of decision variables. The algorithm has been set up with two rounds of calculation: the first one with the initial population selected randomly; the second one with the initial population defined partly randomly and partly with the best individuals found in the first optimization step. This approach allows the algorithm to converge towards a realistic solution of the optimization using the best individuals of the first optimization through the deterministic process of the algorithm. At the same time, the presence of some random individuals allows the algorithm to evolve while maintaining a stochastic component. The goal of the multi-object optimization problem was to minimize the following function:

$$F_i(P) = |1 - \frac{AUCR_{predicted\ i}}{AUCR_{observed\ i}}|$$

where F_i is the fitness function for each $AUCR_{observed\ i}$ (see Tables 1 and 2), and P is the vector of decision variables (CR_{CYP2C8} and IR_{CYP2C8} values for CYP2C8 and values of CR_{CYP2B6}, IR_{CYP2B6} and IC_{CYP2B6} for CYP2B6). The aim of the optimization is to find the values of decision variables that minimize the difference between the experimental AUCR ($AUCR_{observed}$) and the calculated AUCR ($AUCR_{predicted}$) for each AUCR

Table 2
Drug-Drug interaction studies used for predicting the interactions caused by CYP2B6 inhibition or induction.

Inhibitor (dose)	Substrate	*Step*	Observed AUC ratio	Reference
Baicalin (500 mg TID x 14 days)	Bupropion	*Step 1*	1.15	Fan et al., 2009
Cimetidine (800 mg QD)	Bupropion	*Step 1*	1.05	Kustra et al., 1999
Clopidrogrel (75 mg QD x 4 days)	Bupropion	*Step 2*	1.36	Turpeinen et al., 2005
Clopidrogrel (75 mg QD x 4 days)	Efavirenz	*Step 1*	1.26	Jiang et al., 2013
Disulfiram (250 mg QD x 4 days)	Efavirenz	*Step 1*	1.41	McCance-Katz et al., 2014
Hormone replacement therapy (2 mg estradiol valerate and 250 μg levonorgestrel QD x 10 days)	Bupropion	*Step 2*	1.07	Palovaara et al., 2003
MDMA (125 mg SD)	Bupropion	*Step 1*	1.28	Schmid et al., 2015
Nelfinavir (1250 mg BID)	Bupropion	*Step 1*	1.10	Kirby et al., 2011
Prasugrel (10 mg QD)	Bupropion	*Step 1*	1.18	FDA, 2010
Rolapitant (180 mg SD)	Efavirenz	*Step 1*	1.32	Wang et al., 2019
Ticlopidine (250 mg BID x 4 days)	Bupropion	*Step 1*	1.61	Turpeinen et al., 2005
Ticlopidine (250 mg BID)	Ketamine	*Step 1*	2.41	Peltoniemi et al., 2011
Ticlopidine (250 mg BID)	R-methadone	*Step 2*	1.18	Kharasch & Stubbert, 2013
Ticlopidine (250 mg BID)	S-methadone	*Step 1*	1.62	Kharasch & Stubbert, 2013
Voriconazole (400/200 mg BID x 9 days)	Efavirenz	*Step 1*	1.83	Desta et al., 2016
Inducer	**Substrate**	***Step***	**Observed AUC ratio**	**Reference**
Carbamazepine (400 mg × 21 days)	Efavirenz	*Step 1*	0.64	Ji et al., 2008
Cenobamate (200 mg QD x 98 days)	Bupropion	*Step 2*	0.61	FDA, 2019b
Efavirenz (600 mg QD x 15 days)	Bupropion	*Step 1*	0.45	Robertson et al., 2008
Efavirenz (600 mg × 30 days)	R-methadone	*Step 1*	0.45	Kharasch et al., 2012
Efavirenz (600 mg × 30 days)	S-methadone	*Step 1*	0.31	Kharasch et al., 2012
Ezetimibe (10 mg × 11 days)	Efavirenz	*Step 2*	0.91	Fahmi et al., 2016
Ferulic acid (50 mg TID x 14 days)	Bupropion	*Step 1*	0.77	Gao et al., 2013
Indinavir (1200 mg × 7 days)	Efavirenz	*Step 1*	0.81	Fahmi et al., 2016
Isavuconazole (200 mg TID x 11 days)	Bupropion	*Step 1*	0.59	Yamazaki et al., 2017
Itraconazole (200 mg × 6 days)	Efavirenz	*Negative control*	1	Fahmi et al., 2016
Ledipasvir/sofosbuvir (90 mg/400 mg QD x 14 days)	Efavirenz	*Step 1*	0.79	FDA, 2014b
Lopinavir/Ritonavir (400 mg/100 mg BID x 14 days)	Bupropion	*Step 2*	0.43	Hogeland et al., 2007
Metamizole (500 mg TID x 4 days)	Bupropion	*Step 1*	0.67	Qin et al., 2012
Nelfinavir (1250 mg BID x 14 days)	Bupropion	*Step 2*	0.92	Kirby et al., 2011
Nelfinavir (1250 mg BID x 32 weeks)	Efavirenz	*Step 1*	0.83	Fahmi et al., 2016
Nevirapine (200–400 mg × 4 weeks)	Efavirenz	*Step 1*	0.71	Veldkamp et al., 2001
Rifampin (450 mg × 7 days)	Efavirenz	*Step 2*	0.61	Fahmi et al., 2016
Rifampin (600 mg QD x 7 days)	Bupropion	*Step 2*	0.34	Chung et al., 2011
Rifampin (600 mg QD x 7 days)	Bupropion	*Step 1*	0.33	Loboz et al., 2006
Rifampin (600 mg QD x 11 days)	Efavirenz	*Step 2*	0.44	Cho et al., 2016
Ritonavir (100 mg × 23 days)	Bupropion	*Step 1*	0.78	Fahmi et al., 2016
Ritonavir (300 mg BID x 3 days)	Bupropion	*Step 1*	0.84	Kharasch, Bedynek, et al., 2008
Ritonavir (300 mg BID x 3 days)	R-methadone	*Step 2*	0.68	Kharasch, Mitchell, et al., 2008
Ritonavir (300 mg BID x 3 days)	S-methadone	*Step 2*	0.57	Kharasch, Mitchell, et al., 2008
Ritonavir (400 mg BID x 14 days)	R-methadone	*Step 2*	0.51	Kharasch, Mitchell, et al., 2008
Ritonavir (400 mg BID x 14 days)	S-methadone	*Step 2*	0.50	Kharasch, Mitchell, et al., 2008
Ritonavir (400 mg BID x 18 days)	Bupropion	*Step 1*	0.67	Kharasch, Mitchell, et al., 2008
Ritonavir (600 mg BID x 23 days)	Bupropion	*Step 1*	0.34	Park et al., 2010
Saquinavir (1600 mg)	Efavirenz	*Step 1*	0.89	Fahmi et al., 2016
St. John's wort (300 mg TID x 14 days)	Ketamine	*Step 1*	0.40	Peltoniemi et al., 2012
St. John's wort (300 mg TID x 14 days)	Bupropion	*Step 2*	0.83	Lei et al., 2010
Teriflunomide (14–70 mg × 14 days)	Bupropion	*Step 1*	0.91	Fahmi et al., 2016
Tipranavir/Ritonavir (200 mg BID)	Bupropion	*Step 1*	0.54	Younis et al., 2019

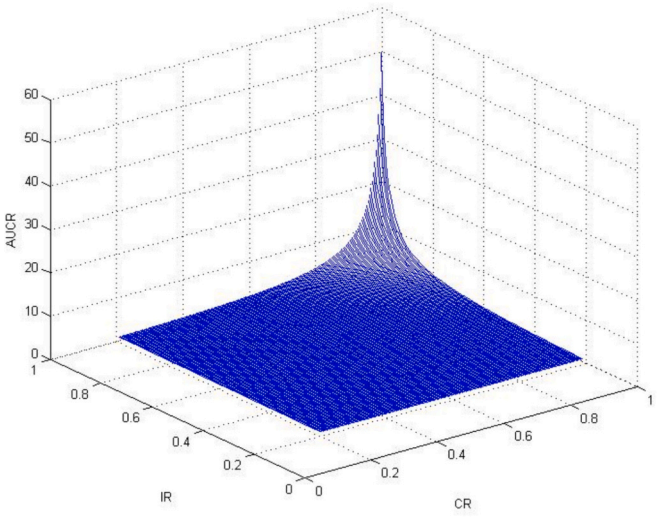

Fig. 1. Genetic algorithm (GA) constraints for enzyme inhibition-based drug-drug interactions (DDIs). Constraints, obtained with the MATLAB software by plotting Eq. (1), used to guide the GA for initial estimation of contribution ratio (CR) and inhibition ratio (IR) values to predict DDIs caused by CYP2B6 or CYP2C8 inhibition.

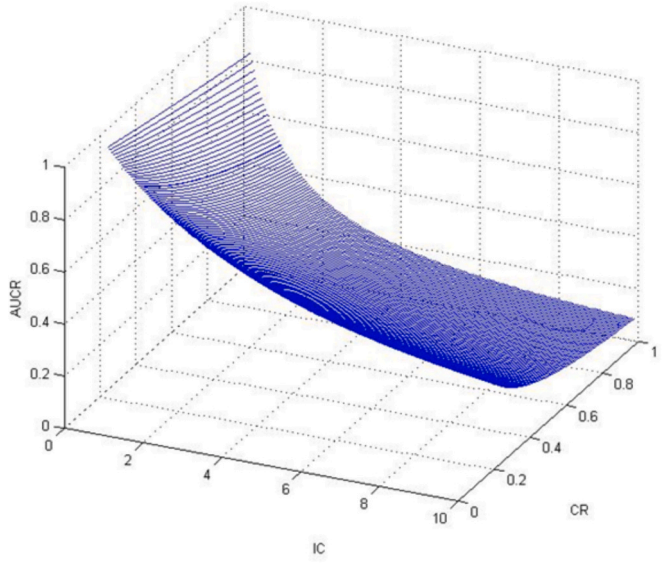

Fig. 2. Genetic algorithm (GA) constraints for enzyme induction-based drug-drug interactions (DDIs). Constraints, obtained with the MATLAB software by plotting Eq. (2), used to guide the GA for initial estimation of contribution ratio (CR) and increases in drug clearance (IC) values to predict DDIs caused by CYP2B6 induction.

that has been considered in the initial estimation step. In the GA algorithm the following parameters were adopted: i) population size of each generation in the optimization run: 300 individuals, ii) maximum generation: 200 individuals; crossover probability (i.e., probability that genes from selected parents produce offspring of the next generation): 0.8 for the first round and 0.9 for the second round.

More information about the computational approach with GA is available in the flowchart of Fig. 3.

2.2. Step 2: external validation of predicted values

The predicted $AUCR_{CYP2B6/CYP2C8}$ values were calculated by solving Eqs. (1) and (2), where the estimates of CR_{CYP2B6}, IR_{CYP2B6}, and IC_{CYP2B6} (for DDIs involving CYP2B6) and CR_{CYP2C8}, and IR_{CYP2C8} (for DDIs involving CYP2C8) were generated by GA in Step 1 (see the DDI studies reported in Tables 1 and 2 as Step 1). Afterwards, the parameters values were used to compare predicted and observed AUCRs obtained from a second set of published articles used as external validation (Step 2 in Tables 1 and 2). This comparison was based on the visual inspection of the graph obtained by plotting predicted versus observed AUCRs. The predicted values were considered correct if 90% of the predicted AUCRs were within range between 50 and 200% of the observed AUCRs (Ohno et al., 2007; Ohno et al., 2008). In addition, the predicted values were compared with the modified ranges proposed by Guest et al. (Guest et al., 2011), typically used for these prediction approaches. The prediction errors (difference between the predicted and the observed value) and the absolute mean of the prediction error were also calculated to indicate the imprecision of the prediction.

2.3. Step 3: final estimation of model parameters

As in previous works (Di Paolo et al., 2021 and references therein), refined estimates of the parameters were obtained through a Bayesian orthogonal regression using the WinBUGS software (version 1.4.3).

For each CYP2B6 or CYP2C8 substrate (χ) and inhibitor (ψ), the predicted AUCR was coded in Winbugs according to Eq. (3):

$$pred_{\chi\psi} = \frac{1}{\left(1 - CRZ_{\chi} \times IRZ_{\psi}\right)} \tag{3}$$

$$AUCratio_{\chi\psi} \sim N\left(pred_{\chi\psi}, tauAUC\right)$$

where $pred_{\chi\psi}$ and $AUCratio_{\chi\psi}$ are the predicted and observed AUCRs for each CR/IR pair, respectively, and CRZ_{χ} and IRZ_{ψ} are the Bayesian posterior values (refined estimates) of the $CR_{CYP2B6/CYP2C8}$ and $IR_{CYP2B6/CYP2C8}$, respectively. *tauAUC* is the precision of the AUC distribution, calculated as the reciprocal of the variance. Normal distribution was assumed for AUCRs, while logistic distribution (between 0 and 1) was assumed for CR_{CYP2C8}, CR_{CYP2B6}, IR_{CYP2C8} and IR_{CYP2B6} values. The mean of each distribution was the initial estimation obtained from Step 1. The precision of the distributions was assumed to obey a gamma distribution: $tauCR \sim (4,1)$; $tauIR \sim G(4,1)$; $tauAUC \sim G(2,1)$. The gamma distributions were set so that the expected standard errors of $CR_{CYP2B6/CYP2C8}$ and $IR_{CYP2B6/CYP2C8}$ values on the logit scale and of AUCRs were 0.5, 0.5 and 5, respectively.

A similar Bayesian regression analysis was applied for the final estimation of parameters related to CYP2B6 induction. The CRs of CYP2B6 were fixed at values obtained from CYP2B6 inhibition data (CRZ_{χ}). Eq. (4) was applied for the regression of each substrate (χ) and inducer (ω):

$$pred_{\chi\omega} = \frac{1}{\left(1 + CRZ_{\chi} \times ICZ_{\omega}\right)} \tag{4}$$

$$AUCratio_{\chi\omega} \sim N\left(pred_{\chi\omega}, tauAUC\right)$$

where $pred_{\chi\omega}$ and $AUCratio_{\chi\omega}$ are the predicted and observed AUCR for each CR_{CYP2B6} and IC_{CYP2B6} pair, respectively; while ICZω is the Bayesian posterior value (final estimation) of ICCYP2B6 values. IC_{CYP2B6} is a positive real number, therefore a log-normal distribution is assumed. The tauAUC precision obeyed gamma distribution, as for inhibition ($tauAUC \sim (2,1)$). The posterior distributions of all estimated parameters CRs, IRs, ICs and AUCRs were obtained from Monte Carlo Markov chain simulation (Winbugs 1.4.3 software). The means of posterior distributions were considered as point estimates of CR_{CYP2B6}, CR_{CYP2C8}, IR_{CYP2B6}, IR_{CYP2C8}, IC_{CYP2B6}, $AUCR_{CYP2B6}$ and $AUCR_{CYP2C8}$ values with 95% confidence intervals. Convergence is evaluated by monitoring the stability of the posterior distributions. The goodness of fit was assessed by visual check of residual scatterplots and posterior distribution.

Finally, to evaluate the success of predictions of DDIs caused by CYP2B6 or CYP2C8 inhibition or CYP2B6 induction, all predicted AUCRs were plotted versus observed AUCRs and compared with Guest ranges (Guest et al., 2011).

3. Results

The computational model presented here was developed to predict DDIs caused by inhibition of CYP2C8 or by induction or inhibition of CYP2B6. Accordingly, a total of 98 studies were used for the final estimation of the relevant parameters CR_{CYP2B6}, CR_{CYP2C8}, IR_{CYP2B6}, IR_{CYP2C8} and IC_{CYP2B6}.

The initial estimates of the parameters (Step 1) are the results of the optimization of the fitness function obtained using a GA. The verification of the estimates generated by the GA-based framework was possible through the external validation in which the predicted $AUCR_{CYP2B6/CYP2C8}$ values versus the observed $AUCR_{CYP2B6/CYP2C8}$ values were plotted (Figs. 4 and 5). All predicted $AUCR_{CYP2B6/CYP2C8}$ values were in the 50–200% of the observed ratio; this finding indicates that the method had a reliable predictive performance. The final parameters and their respective 95% confidence intervals for substrates and inhibitors of CYP2C8 and CYP2B6 and for inducers of CYP2B6 are given in Tables 3–7.

The relationships between the predicted and observed $AUCR_{CYP2B6}$ and $AUCR_{CYP2C8}$ values for all victim drugs are plotted in Figs. 6 and 7. The results obtained demonstrate the good ability of the proposed computational method to predict DDIs elicited by CYP2C8 or CYP2B6

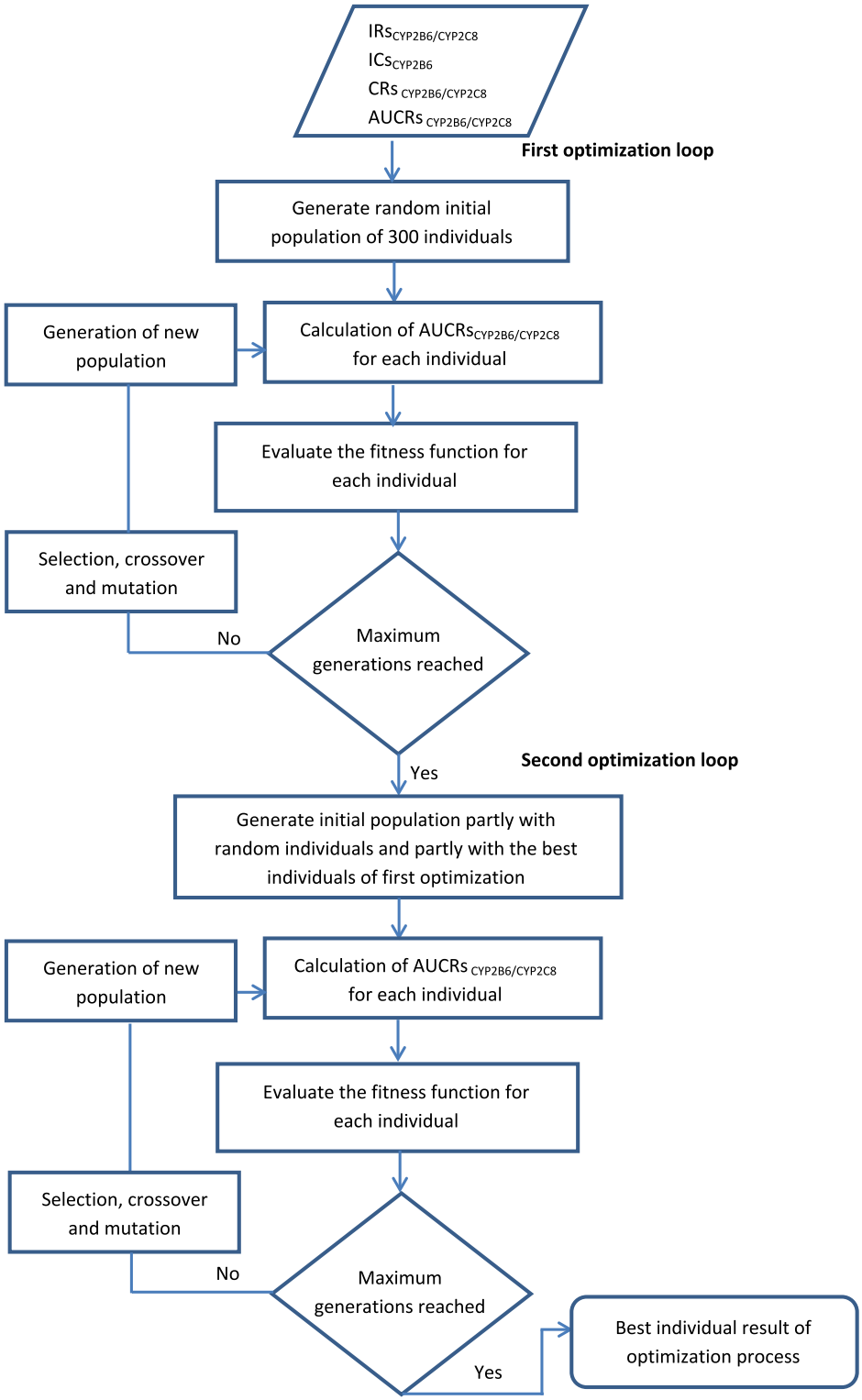

Fig. 3. Genetic Algorithm (GA) Flowchart.

inhibition, or induction of CYP2B6.

4. Discussion

The prediction of DDIs is of great interest to the scientific community due to its significant clinical relevance. Indeed, DDIs are among the main causes compromising the success of a drug therapy and are sometimes responsible for serious adverse events (Ferdousi et al., 2017) being a significant cause of hospital visits and hospital admissions (Dechanont et al., 2014). This study applies a static semi-physiological framework to predict potential DDIs after co-administration of a CYP2B6 or CYP2C8 substrate with inhibitors or inducers (only in the case of CYP2B6) of the same enzyme.

A strength of the approach adopted in this paper, which is based on the framework previously proposed by Ohno et al. (Ohno et al., 2007; Ohno et al., 2008), is that, unlike other modeling approaches that have

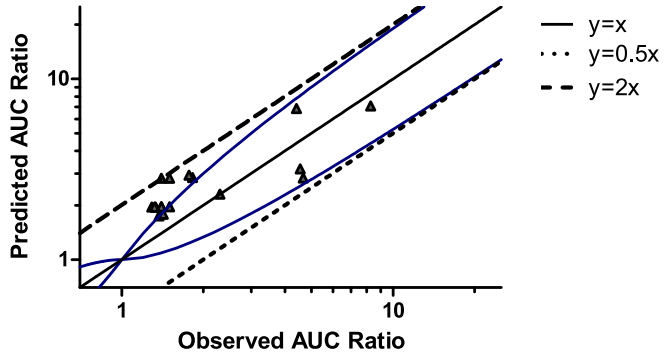

Fig. 4. External validation: predicted versus observed AUC ratios used for prediction of CYP2C8-mediated drug-drug interactions (DDIs). Solid blue curves denote intervals as suggested by Guest et al. (Guest et al., 2011). The solid gray line is the identity line (y = x). The top and the lower dashed lines represent y = 2× and y = 0.5×, respectively. Linear regression analysis led to the following equation: y = 0.6989× + 1.1638 (r^2 = 0.6940).
AUC: area under the plasma concentration-time curve.
r^2: coefficient of determination. (For interpretation of the references to colour in this figure legend, the reader is referred to the web version of this article.)

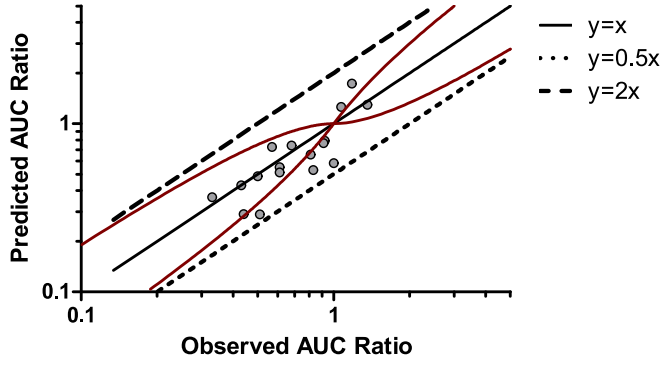

Fig. 5. External validation: predicted versus observed AUC ratios used for prediction of CYP2B6-mediated drug-drug interactions (DDIs). Solid red curves denote intervals as suggested by Guest et al. (Guest et al., 2011). The solid gray line is the identity line (y = x). The top and the lower dashed lines represent y = 2× and y = 0.5×, respectively. Linear regression analyses led to the following equation: y = 1.1124× – 0.1291 (r^2 = 0.6969).
AUC: area under the plasma concentration-time curve.
r^2: coefficient of determination. (For interpretation of the references to colour in this figure legend, the reader is referred to the web version of this article.)

Table 3
Final estimates of CYP2B6 contribution ratios (CR_{CYP2B6}) of CYP2B6 substrates.

Substrate	CR_{CYP2B6}	95% CI
Bupropion	0.41	0.18–0.69
Efavirenz	0.56	0.29–0.81
Ketamine	0.62	0.35–0.85
R-Methadone	0.58	0.32–0.83
S-Methadone	0.63	0.36–0.86

been proposed to predict the extent of potential DDIs, it is based solely on in vivo clinical data, avoiding many of the complexities potentially present in the translation between non-clinical in vivo/in vitro assessments and the relevant human clinical situation (Yoshida et al., 2017). A further strength of our approach is the use of a GA, an evolutionary computation technique which is adopted in various scientific fields for optimization or search problems (among which, e.g., biology, chemistry and engineering) for its high accuracy and simplicity (Alhijawi & Arafat, 2023; Tabassum & Digital, 2014). The GA is less complex than other

Table 4
Final estimates of CYP2B6 inhibition ratios (IR_{CYP2B6}) of CYP2B6 inhibitors.

Inhibitor	IR_{CYP2B6}	95% CI
Baicalin (500 mg TID x 14 days)	0.81	0.60–0.94
Cimetidine (800 mg QD)	0.68	0.43–0.88
Clopidrogrel (75 mg QD x 4 days)	0.57	0.30–0.82
Disulfiram (250 mg QD x 4 days)	0.63	0.37–0.86
Hormone replacement therapy (2 mg estradiol valerate and 250 μg levonorgestrel QD x 10 days)	0.51	0.25–0.78
MDMA (125 mg SD)	0.43	0.19–0.71
Nelfinavir (1250 mg BID)	0.51	0.25–0.78
Prasugrel (10 mg QD)	0.45	0.21–0.73
Rolapitant (180 mg SD)	0.75	0.52–0.92
Ticlopidine (250 mg BID x 4 days)	0.70	0.45–0.89
Voriconazole (400/200 mg BID x 9 days)	0.85	0.66–0.95

CI: confidence interval; BID: twice daily; QD: once daily; SD: single dose; TID: three times daily.

Table 5
Final estimates of increases in drug clearance (IC_{CYP2B6}) of CYP2B6 inducers.

Inducer	IC_{CYP2B6}	95% CI[a]
Carbamazepine (400 mg × 21 days)	1.70	1.39–2.05
Cenobamate (200 mg QD x 98 days)	2.05	1.68–2.47
Efavirenz (600 mg × 30 days)	3.12	2.55–3.76
Ezetimibe (10 mg × 11 days)	0.55	0.45–0.66
Ferulic acid (50 mg TID x 14 days)	1.31	1.07–1.58
Indinavir (1200 mg × 7 days)	0.95	0.78–1.14
Isavuconazole (200 mg TID x 11 days)	2.05	1.68–2.47
Itraconazole (200 mg × 6 days)	1.29	1.05–1.55
Ledipasvir/sofosbuvir (90 mg/400 mg QD x 14 days)	0.71	0.58–0.86
Lopinavir/Ritonavir (400 mg/100 mg BID x 14 days)	3.33	2.73–4.01
Metamizole (500 mg TID x 4 days)	1.47	1.21–1.77
Nelfinavir (1250 mg BID x 14 days)	0.67	0.54–0.80
Nevirapine (200–400 mg × 4 weeks)	1.71	1.40–2.06
Rifampin (450 mg × 7 days)	1.70	1.39–2.05
Rifampin (600 mg × 7–11 days)	4.39	3.59–5.28
Ritonavir (100 mg × 23 days)	1.29	1.05–1.55
Ritonavir (300 mg BID x 3 days)	0.59	0.49–0.72
Ritonavir (400 mg BID x 18 days)	1.66	1.36–2.00
Ritonavir (600 mg BID x 23 days)	4.18	3.43–5.04
Saquinavir (1600 mg)	0.55	0.45–0.66
St. John's wort (300–325 mg TID x 14 days)	2.23	1.83–2.69
Teriflunomide (14–70 mg × 14 days)	0.45	0.37–0.54
Tipranavir/Ritonavir (200 mg BID)	3.31	2.71–3.98

CI: confidence interval; BID: twice daily; QD: once daily; SD: single dose; TID: three times daily.

Table 6
Final estimates of CYP2C8 contribution ratios (CR_{CYP2C8}) of CYP2C8 substrates.

Substrate	CR_{CYP2C8}	95% CI
Amodiaquine	0.88	0.72–0.96
Cerivastatin (acid)	0.88	0.73–0.96
Cerivastatin (lactone)	0.88	0.73–0.96
Dabrafenib	0.65	0.39–0.87
Daprodustat	0.97	0.92–0.99
Dasabuvir	0.94	0.85–0.98
Enzalutamide	0.80	0.58–0.94
Ezetimibe	0.51	0.25–0.78
Loperamide	0.77	0.54–0.92
Montelukast	0.70	0.45–0.89
Paritaprevir	0.51	0.25–0.78
Pioglitazone	0.66	0.40–0.87
Repaglinide	0.88	0.74–0.97
R-Ibuprofen	0.57	0.30–0.82
Rosiglitazone	0.58	0.32–0.83
Simvastatin (acid)	0.74	0.50–0.91
Simvastatin (lactone)	0.51	0.25–0.78
Sitagliptin	0.51	0.25–0.78
Treprostinil	0.72	0.47–0.90

CI: confidence interval.

Table 7
Final estimates of CYP2C8 inhibition ratios (IR_{CYP2C8}) of CYP2C8 inhibitors.

Inhibitor	IR_{CYP2C8}	95% CI
Abriraterone acetate (1000 mg SD)	0.68	0.41–0.88
Amodiaquine (600 mgSD)	0.57	0.30–0.82
Atazanavir (400 mg QD x 6 days)	0.63	0.36–0,85
Capmatinib (400 mg BID x 10 days)	0.54	0.28–0.80
Clopidrogrel (300 mg then 75 mg QD x 3 days)	0.94	0.86–0.99
Cotrimoxazole (160/800 mg BID x 6 days)*	0.54	0.28–0.80
Deferasirox (30 mg/kg QD X 3 days)	0.71	0.49–0.90
Duvelisib (25 mg BID x 6 days)	0.60	0.33–0.84
Efavirenz (400 mg daily x 12 days)	0.63	0.36–0.85
Fedratinib (400 mg QD x 15 days)	0.39	0.17–0.67
Fluvoxamine (50 mg BID x 3.5 days)	0.60	0.33–0.84
Gemfibrozil (600 mg BID x 3 days)	0.95	0.88–0.99
Irbesartan (300 mg QD x 5 days)	0.54	0.28–0.80
Ketoconazole (400 mg QD x 6 days)	0.49	0.24–0.76
Lesinurad (400 mg SD)	0.54	0.28–0.80
Letermovir (480 mg QD x 10 days)	0.64	0.38–0.86
Rolapitant (200 mg SD)	0.65	0.39–0.87
Tazemetostat (800 mg BID at steady state)	0.72	0.47–0.90
Tecovirimat (600 mg BID x 15 days)	0.54	0.28–0.80
Telithromycin (800 mg QD x 3 days)	0.72	0.47–0.90
Teriflunomide (14–70 mg QD x 12 days)	0.82	0.62–0.94
Trimethoprim (160–960 mg BID x 6 days)	0.71	0.46–0.90
Tucatinib (300 mg BID x 10 days)	0.61	0.35–0.85

CI: confidence interval; BID: twice daily; QD: once daily; SD: single dose.

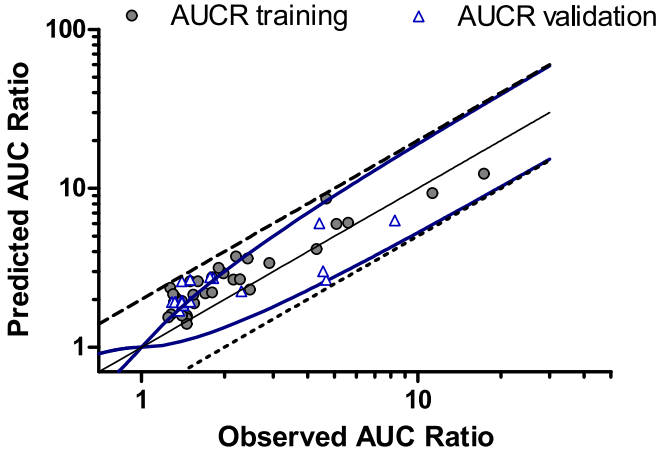

Fig. 6. Predicted versus observed AUC ratios with final estimates of the CYP2C8 contribution ratio (CRs_{CYP2C8}) and CYP2C8 inhibition ratio (IRs_{CYP2C8}). The triangle symbols are predictions from the external validation step; the filled circles are the predictions from the final estimation step. The blue solid curves denote the limits as suggested by Guest et al. (Guest et al., 2011). The gray solid line is the line of identity (y = x). The upper and lower dashed lines represent y = 2 x and y = 0.5×, respectively. AUCR training: drug-drug interaction (DDI) data used for initial estimation of CRs_{CYP2C8} and IRs_{CYP2C8}; AUCR validation: DDI data used for external validation. Linear regression analyses led to the following equation: y = 0.7019× + 1.1904 (r^2 = 0.8429).
AUC: area under the plasma concentration-time curve.
AUCR: AUC ratio.
r^2: coefficient of determination. (For interpretation of the references to colour in this figure legend, the reader is referred to the web version of this article.)

algorithms and, at the same time, its application in different platforms increases its flexibility (Tabassum & Digital, 2014). The power of GAs is to process populations of data, while a traditional method works with a single point. It is known that selecting appropriate initial estimates is important in nonlinear regression to avoid local minima (Alhijawi & Arafat, 2023). During the step 1 of this model development, several rounds of the GA were conducted to avoid local optima solutions. To this end, for the initial estimation of the parameters (i.e., CR_{CYP2C8}, CR_{CYP2B6}, IR_{CYP2C8} IR_{CYP2B6} and IC_{CYP2B6} values) constraints were used

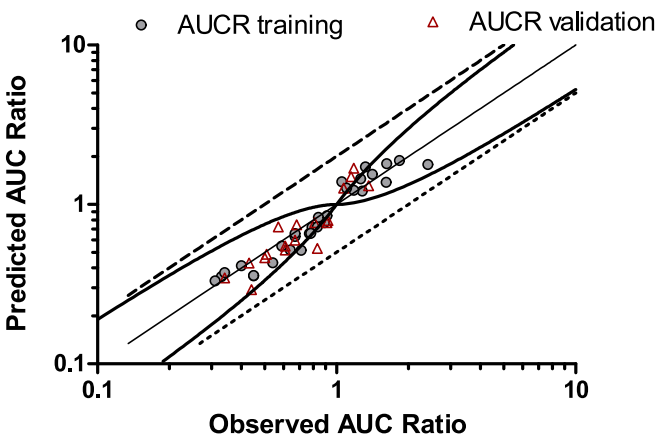

Fig. 7. Predicted versus observed AUC ratios with final estimates of the CYP2B6 contribution ratio (CRs_{CYP2B6}), CYP2B6 inhibition ratio (IRs_{CYP2B6}) and CYP2B6 increases in drug clearance (ICs_{CYP2B6}). The triangle symbols are predictions from the external validation step 2; the filled circles are the predictions from the final estimation step. The black solid curves denote the limits as suggested by Guest et al. (Guest et al., 2011). The gray solid line is the line of identity (y = x). The upper and lower dashed lines represent y = 2 x and y = 0.5×, respectively. AUCR training: drug-drug interaction (DDI) data used for initial estimation of CRs_{CYP2B6}, IRs_{CYP2B6} and ICs_{CYP2B6}; AUCR validation: DDI data used for external validation. Linear regression analyses led to the following equation: y = 0.9977× – 0.006 (r^2 = 0.8463).
AUC: area under the plasma concentration-time curve.
AUCR: AUC ratio.
r^2: coefficient of determination.

to guide the GA in the search for the fittest solutions (Figs. 1 and 2). It is well known that whilst a GA cannot guarantee optimality of the obtained solution, usually the results are close to the global optimum (Sale & Sherer, 2015).

Our approach represents an advancement of the framework proposed by Ohno et al. (Ohno et al., 2007; Ohno et al., 2008) as, due to the use of a GA, it does not require the assumption of any a priori value on any parameter. This aspect is advantageous since, assuming an initial value of CR or IR for a particular DDI may subsequently lead to biased parameters, which, unavoidably, will in turn affect the estimated AUCR predicted values. In addition, the GA approach avoids the perfect prediction phenomenon (i.e., predicted AUCR falling exactly on the identity line with observed AUCR), which is often observed in the standard application of the Ohno et al.'s approach (Di Paolo et al., 2021; Di Paolo et al., 2022), when considering cases in which a drug substrate or a perpetrator was uniquely considered in an individual study.

Overall, the AUC ratios of 5 substrates, 11 inhibitors and 19 inducers of CYP2B6, and the AUC ratios of 19 substrates and 23 inhibitors of CYP2C8 were successfully predicted by this method. It is important to underline that the administration of a substrate drug characterized by a high CR together with an enzyme inhibitor endowed with a high IR, or an enzyme inducer with a high IC represents the situation characterized by the highest risk of significant DDI in the clinical settings. In this regard, the most sensitive substrate of CYP2B6 is S-methadone, with a CR of 0.63 (Table 3); this CR value indicates that other, non-negligible metabolic pathways are also active for this substrate. On the other hand, daprodustat appears to be the most sensitive substrate for CYP2C8. In this case, the CR value of 0.97 (Table 5) indicates that this drug is metabolized almost exclusively by CYP2C8 and may therefore serve as an index substrate for DDIs involving the inhibition of this specific CYP. Furthermore, voriconazole (IR = 0.85) and gemfibrozil (IR = 0.95) are the most potent perpetrators of inhibitory DDIs involving CYP2B6 and CYP2C8, respectively, being able to suppress almost completely the metabolic activity of these enzymes (85 and 95% inhibition, respectively; Tables 4 and 7). Based on Eq. (1), the combination

of daprodustat and gemfibrozil is predicted to provide a large AUCR value of ~13, consistent with the experimental data (17.36, Table 1). In the case of CYP2B6, there is no experimental value for the AUCR related to the DDI of S-methadone with voriconazole; however, with Eq. (1) we can predict an AUCR value of 2.15, which is much lower than the value reported above for daprodustat and gemfibrozil. This is consequence of the fact that S-methadone is a less sensitive substrate of CYP2B6 as compared to daprodustat for CYP2C8. As far as induction of CYP2B6 is concerned, rifampin (600 mg × 7–11 days) was found to be the drug endowed with the highest IC among CYP2B6 inducers (Table 5), and thus has the highest potential to perpetrate significant DDIs with sensitive CYP2B6 substrate drugs (e.g., S-methadone). Induction of CYP2C8 was not considered in this exercise, as there was a limited number of in vivo studies assessing the impact of inducers on drug substrates of this enzyme; in particular, it was cumbersome to properly set the external validation step of the approach. However, an exploration based on the available DDI studies involving CYP2C8 inducers (13 studies involving 4 substrates and 11 inducers; data not shown) was able to correctly identify rifampicin and carbamazepine as the most potent inducers of CYP2C8, without showing large differences in the CR parameters for CYP2C8 substrates compared to those obtained using the full approach from inhibition DDI studies.

It is noteworthy that all the predictions obtained in this work have an accuracy comparable or superior to that previously achieved by our application of the model of Ohno et al. (Di Paolo et al., 2021; Di Paolo et al., 2022), and that the external validation AUC ratios were in the range of 50–200% of the observed value for both CYP2B6- and CYP2C8-based DDIs. Moreover, it is important to note that in many cases (namely, 38 out of 50 predictions of AUC_{CYP2C8} ratios) the proposed GA-based methodology was able to predict values with better accuracy than those previously anticipated (Di Paolo et al., 2021). For example, for the gemfibrozil-cerivastatin interaction the prediction of the AUC ratio obtained by the GA-based approach was ~14% more accurate than that obtained using the model proposed by Ohno et al., being the predicted value equal to 108 and 122% of the observed value, respectively (Di Paolo et al., 2021). The performance of the GA-based method versus the Ohno et al.'s approach was superior for predictions related to CYP2C8 (38 out of 50 more accurate AUC $ratios_{CYP2C8}$) than for predictions related to CYP2B6 (11 out of 48 more accurate AUC $ratios_{CYP2B6}$). This difference could be due to the smaller size of the dataset of substrates of CYP2B6 ($n = 5$) compared to that of CYP2C8 ($n = 19$). Conceivably, a larger number of available DDI data would improve GA's ability to search for solutions through mutation, selection and crossover and thus prediction performance.

In conclusion, the simple GA-based static semi-physiological approach proposed in this paper allows to accurately predict the extent of DDIs involving inhibition of CYP2C8 or CYP2B6, or induction of CYP2B6. The incorporation of a GA in the framework avoids the uncertainty attributed to the initial assumptions that characterize other methods for the prediction of metabolism-based DDIs, including that proposed by Ohno et al. (Ohno et al., 2007; Ohno et al., 2008), of which our approach represents a refinement. The real power of this methodology is that it relies only on the use of in vivo clinical data without the need of assumption of any a priori value on any parameter.

CRediT authorship contribution statement

Veronica Di Paolo: Writing – original draft, Methodology, Investigation, Formal analysis, Data curation, Conceptualization. **Francesco Maria Ferrari:** Writing – original draft, Methodology, Investigation, Formal analysis. **Davide Veronese:** Methodology, Data curation. **Italo Poggesi:** Writing – review & editing, Writing – original draft, Supervision, Methodology, Investigation, Formal analysis, Conceptualization. **Luigi Quintieri:** Writing – review & editing, Writing – original draft, Supervision, Methodology, Investigation, Conceptualization.

Declaration of competing interest

The authors declare the following financial interests/personal relationships which may be considered as potential competing interests:

Italo Poggesi reports a relationship with GlaxoSmithKline SpA that includes: employment and equity or stocks. Italo Poggesi reports a relationship with Janssen-Cilag SpA that includes: employment and equity or stocks. Italo Poggesi reports a relationship with Certara that includes: employment. If there are other authors, they declare that they have no known competing financial interests or personal relationships that could have appeared to influence.

Data availability

Data will be made available on request.

References

Abouir, K., Samer, C. F., Gloor, Y., Desmeules, J. A., & Daali, Y. (2021). Reviewing data integrated for PBPK model development to predict metabolic drug-drug interactions: Shifting perspectives and emerging trends. *Frontiers in Pharmacology, 12*, Article 708299.

Akande AA, Olugbenga SJ, Adebanjo AJ, Toyin AS ad, Ogbona OC (2015). Effects of co-trimoxazole co-administration on the pharmacokinetics of amodiaquine in healthy volunteers. International Journal of Pharmacy and Pharmaceutical Sciences, 7: 272–6.

Alhijawi, B., & Arafat, A. (2023). Genetic algorithms: Theory, genetic operators, solutions, and applications. *Evolutionary Intelligence, 2065*(1), 3. https://doi.org/10.1007/s12065-023-00822-6

Aquilante, C. L., Kosmiski, L. A., Bourne, D. W. A., Bushman, L. R., Daily, E. B., Hammond, K. P., … Sidhom, M. S. (2013). Impact of the CYP2C8 *3 polymorphism on the drug-drug interaction between gemfibrozil and pioglitazone. *British Journal of Clinical Pharmacology, 75*, 217–226.

Arun, K. P., Meda, V. S., Raj Kucherlapati, V. S. P., Dubala, A., Deepalakshmi, M., Anand VijayaKumar, P. R., … Suresh, B. (2012). Pharmacokinetic drug interaction between gemfibrozil and sitagliptin in healthy Indian male volunteers. *European Journal of Clinical Pharmacology, 68*, 709–714.

Backman, J. T., Filppula, A. M., Niemi, M., et al. (2016). Role of cytochrome P450 2C8 indrug metabolism and interactions. *Pharmacological Reviews, 68*, 168–241.

Backman, J. T., Kajosaari, L. I., Neuvonen, M., & Neuvonen, P. J. (2003). Trimethoprim increases the plasma concentrations of cerivastatin by inhibiting its CYP2C8-mediated metabolism, abstract in 8th European ISSX meeting, Dijon, France (April 27-may 1, 2003). *Drug Metabolism Reviews, 35*(Suppl), 1.

Backman, J. T., Kyrklund, C., Kivistö, K. T., Wang, J. S., & Neuvonen, P. J. (2000). Plasma concentrations of active simvastatin acid are increased by gemfibrozil. *Clinical Pharmacology and Therapeutics, 68*, 122–129.

Backman, J. T., Kyrklund, C., Neuvonen, M., & Neuvonen, P. J. (2002). Gemfibrozil greatly increases plasma concentrations of cerivastatin. *Clinical Pharmacology and Therapeutics, 72*, 685–691.

Cho, D. Y., Shen, J. H. Q., Lemler, S. M., Skaar, T. C., Li, L., Blievernicht, J., … Desta, Z. (2016). Rifampin enhances cytochrome P450 (CYP) 2B6-mediated efavirenz 8-hydroxylation in healthy volunteers. *Drug Metabolism and Pharmacokinetics, 31*, 107–116.

Chung, J. Y., Cho, J. Y., Lim, H. S., Kim, J. R., Yu, K. S., Lim, K. S., … Jang, I. J. (2011). Effects of pregnane X receptor (NR1I2) and CYP2B6 genetic polymorphisms on the induction of bupropion hydroxylation by rifampin. *Drug Metabolism and Disposition, 39*, 92–97.

Dechanont, S., Maphanta, S., Butthum, B., & Kongkaew, C. (2014). Hospital admissions/visits associated with drug-drug interactions: A systematic review and meta-analysis. *Pharmacoepidemiology and Drug Safety, 23*, 489–497.

Desta, Z., Metzger, I. F., Thong, N., Lu, J. B. L., Callaghan, J. T., Skaar, T. C., … Galinsky, R. E. (2016). Inhibition of cytochrome P450 2B6 activity by voriconazole profiled using efavirenz disposition in healthy volunteers. *Antimicrobial Agents and Chemotherapy, 60*, 6813–6822.

Di Paolo, V., Ferrari, F. M., Poggesi, I., & Quintieri, L. (2021). A quantitative approach to the prediction of drug-drug interactions mediated by cytochrome P450 2C8 inhibition. *Expert Opinion on Drug Metabolism & Toxicology, 17*, 1345–1352.

Di Paolo, V., Ferrari, F. M., Poggesi, I., & Quintieri, L. (2022). Quantitative prediction of drug interactions caused by cytochrome P450 2B6 inhibition or induction. *Clinical Pharmacokinetics, 61*, 1297–1306.

Dong, Y., & Peng, J. (2011). Automatic generation of software test cases based on improved genetic algorithm. In *International conference on multimedia technology*. IEEE. https://ieeexplore.ieee.org/abstract/document/6002999/.

Edema, O., Adeagbo, B. A., Adehin, A., & Olugbade, T. A. (2018). Bidirectional pharmacokinetic interaction between amodiaquine and pioglitazone in healthy subjects. *Journal of Clinical Pharmacology, 58*, 1061–1066.

Fahmi, O. A., Shebley, M., Palamanda, J., Sinz, M. W., Ramsden, D., Einolf, H. J., … Wang, H. (2016). Evaluation of CYP2B6 induction and prediction of clinical drug-drug interactions: Considerations from the IQ consortium induction working group-an industry perspective. *Drug Metabolism and Disposition, 44*, 1720–1730.

Fan, L., Wang, J. C., Jiang, F., Tan, Z. R., Chen, Y., Li, Q., … Zhou, H. H. (2009). Induction of cytochrome P450 2B6 activity by the herbal medicine baicalin as measured by bupropion hydroxylation. *European Journal of Clinical Pharmacology, 65*, 403–409.

FDA (2010). Center for drug evaluation and research, administrative and correspondence documents. https://www.accessdata.fda.gov/drugsatfda_docs/nda/2010/201023Orig1s000Admincorres.pdf.

FDA (2014b). Center for drug evaluation and clinical pharmacology and biopharmaceutics. review(s).https://www.accessdata.fda.gov/drugsatfda_docs/nda/2014/205834Orig1s000ClinPharmR.pdf.

FDA. (2009). Centre for drug evaluation and research: Clinical pharmacology and biopharmaceutics review(s): Tyvaso. http://www.accessdata.fda.gov/drugsatfda_docs/nda/2009/022387s000ClinPharmR.pdf.

FDA. (2012). Center for drug evaluation and research Clinical Pharmacology and biopharmaceutics review(s). https://www.accessdata.fda.gov/drugsatfda_docs/nda/2012/202992Orig1s000ClinpharmR.pdf.

FDA. (2014). Center for drug evaluation and research chemistry review (s). https://accessdata.fda.gov/drugsatfda_docs/nda/2014/206619Orig1s000ChemR.pdf.

FDA. (2015a). Center for drug evaluation and research highlights of prescribing information. https://www.accessdata.fda.gov/drugsatfda_docs/label/2015/021567s037,206352s002lbl.pdf.

FDA. (2015b). Center for drug evaluation and research summary review. https://www.accessdata.fda.gov/drugsatfda_docs/nda/2015/207988Orig1s000SumR.pdf.

FDA. (2015c). Center for drug evaluation and research summary review. https://www.accessdata.fda.gov/drugastfda_docs/nda/2015/206500Orig1s000SumR.pdf.

FDA. (2017). Center for drug evaluation and research summary review. https://www.accessdata.fda.gov/drugsatfda_docs/nda/2017/209939Orig1s000,209940Orig1s000SumR.pdf.

FDA. (2018a). Center for drug evaluation and research administrative and correspondence documents. https://www.accessdata.fda.gov/drugsatfda_docs/nda/2018/211155-Orig1Orig2s000AdminCorres.pdf.

FDA. (2018b). Center for drug evaluation and research summary review. https://www.accessdata.fda.gov/drugsatfda_docs/nda/2018/208627Orig1s000SumR.pdf.

FDA. (2019a). Center for drug evaluation and research application number: 761128Orig1s000 multi-discipline review Summary review office director cross discipline team leader review clinical review non-clinical review statistical review clinical pharmacology review. https://www.accessdata.fda.gov/drugsatfda_docs/nda/2019/212526Orig1s000MultidisciplineR.pdf.

FDA. (2019b). Center for drug evaluation and research application number: 212839Orig1s000 other review(s). https://www.accessdata.fda.gov/drugsatfda_docs/nda/2019/212839Orig1s000OtherR.pdf.

FDA. (2020a). Center for drug evaluation and research multi-discipline review. https://www.accessdata.fda.gov/drugsatfda_docs/nda/2019/212327Orig1s000MultidisciplineR.pdf.

FDA. (2020b). Center for drug evaluation and research multi-discipline review. https://www.accessdata.fda.gov/drugsatfda_docs/nda/2020/213591Orig1s000MultidisciplineR.pdf.

Ferdousi, R., Safdari, R., & Omidi, Y. (2017). Computational prediction of drug-drug interactions based on drugs functional similarities. *Journal of Biomedical Informatics, 70*, 54–64.

Ferreira, L. L., & Andricopulo, A. D. (2019). ADMET modeling approaches in drug discovery. *Drug Discovery Today, 24*, 1157–1165.

Gao, L., He, Y., Tang, J., Yin, J., Huang, Z., Liu, F., … Zhou, H. (2013). Genetic variants of Pregnane X receptor (PXR) and CYP2B6 affect the induction of bupropion hydroxylation by sodium Ferulate. *PLoS One, 8*.

Gaurav, D., Rodriguez, F. O., Tiwari, S., & Jabbar, M. A. (2021). Review of machine learning approach for drug development process. In *Deep learning in biomedical and health informatics* (pp. 53–77). CRC Press.

Gibbons, J. A., de Vries, M., Krauwinkel, W., Ohtsu, Y., Noukens, J., van der Walt, J. S., … Ouatas, T. (2015). Pharmacokinetic drug interaction studies with enzalutamide. *Clinical Pharmacokinetics, 54*, 1057–1069.

Guest, E. J., Aarons, L., Houston, J. B., Rostami-Hodjegan, A., & Galetin, A. (2011). Critique of the two-fold measure of prediction success for ratios: Application for the assessment of drug-drug interactions. *Drug Metabolism and Disposition, 39*, 170–173.

Han, K., Cao, P., Wang, Y., Xie, F., Ma, J., Yu, M., … Wan, J. (2022). A review of approaches for predicting drug-drug interactions based on machine learning. *Frontiers in Pharmacology, 12*, Article 814858.

Hogeland, G. W., Swindells, S., McNabb, J. C., Kashuba, A. D. M., Yee, G. C., & Lindley, C. M. (2007). Lopinavir/ritonavir reduces bupropion plasma concentrations in healthy subjects. *Clinical Pharmacology and Therapeutics, 81*, 69–75.

Holland, J. H. (1992). *Scientific American genetic algorithms. 267* pp. 66–73).

Honkalammi, J., Niemi, M., Neuvonen, P. J., & Backman, J. T. (2011). Dose-dependent interaction between gemfibrozil and repaglinide in humans: Strong inhibition of CYP2C8 with subtherapeutic gemfibrozil doses. *Drug Metabolism and Disposition, 39*, 1977–1986.

Itkonen, M. K., Tornio, A., Filppula, A. M., Neuvonen, M., Neuvonen, P. J., Niemi, M., & Backman, J. T. (2018). Clopidogrel but not Prasugrel significantly inhibits the CYP2C8-mediated metabolism of Montelukast in humans. *Clinical Pharmacology and Therapeutics, 104*, 495–504.

Itkonen, M. K., Tornio, A., Lapatto-Reiniluoto, O., Neuvonen, M., Neuvonen, P. J., Niemi, M., & Backman, J. T. (2019). Clopidogrel increases dasabuvir exposure with or without ritonavir, and ritonavir inhibits the bioactivation of clopidogrel. *Clinical Pharmacology and Therapeutics, 105*, 219–228.

Itkonen, M. K., Tornio, A., Neuvonen, M., Neuvonen, P. J., Niemi, M., & Backman, J. T. (2016). Clopidogrel markedly increases plasma concentrations of CYP2C8 substrate pioglitazone. *Drug Metabolism and Disposition, 44*, 1364–1371.

Ji, P., Damle, B., Xie, J., Unger, S. E., Grasela, D. M., & Kaul, S. (2008). Pharmacokinetic interaction between efavirenz and carbamazepine after multiple-dose administration in healthy subjects. *Journal of Clinical Pharmacology, 48*, 948–956.

Jiang, F., Desta, Z., Shon, J. H., Yeo, C. W., Kim, H. S., Liu, K. H., … Shin, J. G. (2013). Effects of clopidogrel and itraconazole on the disposition of efavirenz and its hydroxyl metabolites: Exploration of a novel CYP2B6 phenotyping index. *British Journal of Clinical Pharmacology, 75*, 244–253.

Johnson, B. M., Stier, B. A., & Caltabiano, S. (2014). Effect of food and gemfibrozil on the pharmacokinetics of the novel prolyl hydroxylase inhibitor GSK1278863. *Clinical Pharmacology in Drug Development, 3*, 109–117.

Kajosaari, L. I., Niemi, M., Backman, J. T., & Neuvonen, P. J. (2006). Telithromycin, but not montelukast, increases the plasma concentrations and effects of the cytochrome P450 3A4 and 2C8 substrate repaglinide. *Clinical Pharmacology and Therapeutics, 79*, 231–242.

Karonen, T., Filppula, A., Laitila, J., Niemi, M., Neuvonen, P. J., & Backman, J. T. (2010). Gemfibrozil markedly increases the plasma concentrations of montelukast: A previously unrecognized role for CYP2c8 in the metabolism of montelukast. *Clinical Pharmacology and Therapeutics, 88*, 223–230.

Kharasch, E. D., Bedynek, P. S., Park, S., Whittington, D., Walker, A., & Hoffer, C. (2008). Mechanism of ritonavir changes in methadone pharmacokinetics and pharmacodynamics: I. Evidence against CYP3A mediation of methadone clearance. *Clinical Pharmacology and Therapeutics, 84*, 497–505.

Kharasch, E. D., Mitchell, D., Coles, R., & Blanco, R. (2008). Rapid clinical induction of hepatic cytochrome P4502B6 activity by ritonavir. *Antimicrobial Agents and Chemotherapy, 52*, 1663–1669.

Kharasch, E. D., & Stubbert, K. (2013). Role of cytochrome P4502B6 in methadone metabolism and clearance. *Journal of Clinical Pharmacology, 53*, 305–313.

Kharasch, E. D., Whittington, D., Ensign, D., Hoffer, C., Bedynek, P. S., Campbell, S., … Kim, T. (2012). Mechanism of efavirenz influence on methadone pharmacokinetics and pharmacodynamics. *Clinical Pharmacology and Therapeutics, 91*, 673–684.

Kim, S. J., Yoshikado, T., Ieiri, I., Maeda, K., Kimura, M., Irie, S., … Sugiyama, Y. (2016). Clarification of the mechanism of clopidogrel-mediated drug-drug interaction in a clinical cassette small-dose study and its prediction based on in vitro information. *Drug Metabolism and Disposition, 44*, 1622–1632.

Kirby, B. J., Collier, A. C., Kharasch, E. D., Dixit, V., Desai, P., Whittington, D., … Unadkat, J. D. (2011). Complex drug interactions of HIV protease inhibitors 2: In vivo induction and in vitro to in vivo correlation of induction of cytochrome P450 1A2, 2B6, and 2C9 by ritonavir or nelfinavir. *Drug Metabolism and Disposition, 39*, 2329–2337.

Kramer, O. (2017). Genetic algorithms. *Stud Comput Intell, 679*, 11–19.

Kustra, R., Corrigan, B., Dunn, J., Duncan, B., & Hsyu, P.-H. (1999). Lack of effect of cimetidine on the pharmacokinetics of sustained-release bupropion. *Journal of Clinical Pharmacology, 39*, 1184–1188.

Lei, H. P., Yu, X. Y., Xie, H. T., Li, H. H., Fan, L., Dai, L. L., … Zhou, H. H. (2010). Effect of St. John's wort supplementation on the pharmacokinetics of bupropion in healthy male Chinese volunteers. *Xenobiotica, 40*, 275–281.

Loboz, K. K., Gross, A. S., Williams, K. M., Liauw, W. S., Day, R. O., Blievernicht, J. K., … McLachlan, A. J. (2006). Cytochrome P450 2B6 activity as measured by bupropion hydroxylation: Effect of induction by rifampin and ethnicity. *Clinical Pharmacology and Therapeutics, 80*, 75–84.

McCance-Katz, E. F., Gruber, V. A., Beatty, G., Lum, P., Ma, Q., Difrancesco, R., … Morse, G. D. (2014). Interaction of disulfiram with antiretroviral medications: Efavirenz increases while atazanavir decreases disulfiram effect on enzymes of alcohol metabolism. *The American Journal on Addictions, 23*, 137–144.

Menon, R. M., Badri, P. S., Wang, T., Polepally, A. R., Zha, J., Khatri, A., et al. (2015). Drug-drug interaction profile of the all-oral anti-hepatitis C virus regimen of paritaprevir/ritonavir, ombitasvir, and dasabuvir. *Journal of Hepatology, 63*, 20–29.

Monbaliu, J., Gonzalez, M., Bernard, A., Jiao, J., Sensenhauser, C., Snoeys, J., … Chien, C. (2016). In vitro and in vivo drug-drug interaction studies to assess the effect of abiraterone acetate, abiraterone, and metabolites of abiraterone on CYP2C8 activity. *Drug Metabolism and Disposition, 44*, 1682–1691.

Niemi, M., Backman, J. T., Granfors, M., Laitila, J., Neuvonen, M., & Neuvonen, P. J. (2003). Gemfibrozil considerably increases the plasma concentrations of rosiglitazone. *Diabetologia, 46*, 1319–1323.

Niemi, M., Backman, J. T., & Neuvonen, P. J. (2004). Effects of trimethoprim and rifampin on the pharmacokinetics of the cytochrome P450 2C8 substrate rosiglitazone. *Clinical Pharmacology and Therapeutics, 76*, 239–249.

Niemi, M., Tornio, A., Pasanen, M. K., Fredrikson, H., Neuvonen, P. J., & Backman, J. T. (2006). Itraconazole, gemfibrozil and their combination markedly raise the plasma concentrations of loperamide. *European Journal of Clinical Pharmacology, 62*, 463–472.

Ohno, Y., Hisaka, A., & Suzuki, H. (2007). General framework for the quantitative prediction of CYP3A4-mediated oral drug interactions based on the AUC increase by coadministration of standard drugs. *Clinical Pharmacokinetics, 46*, 681–696.

Ohno, Y., Hisaka, A., Ueno, M., & Suzuki, H. (2008). General framework for the prediction of oral drug interactions caused by CYP3A4 induction from in vivo information. *Clinical Pharmacokinetics, 47*, 669–680.

Palovaara, S., Pelkonen, O., Uusitalo, J., Lundgren, S., & Laine, K. (2003). Inhibition of cytochrome P450 2B6 activity by hormone replacement therapy and oral contraceptive as measured by bupropion hydroxylation. *Clinical Pharmacology and Therapeutics, 74*, 326–333.

Park, J., Vousden, M., Brittain, C., McConn, D. J., Iavarone, L., Ascher, J., … Muir, K. T. (2010). Dose-related reduction in bupropion plasma concentrations by ritonavir. *Journal of Clinical Pharmacology, 50*, 1180–1187.

Park, J. Y., Kim, K. A., Shin, J. G., & Lee, K. Y. (2004). Effect of ketoconazole on the pharmacokinetics of rosiglitazone in healthy subjects. *British Journal of Clinical Pharmacology, 58*, 397–402.

Pedersen, R. S., Damkier, P., & Brosen, K. (2006). The effects of human CYP2C8 genotype and fluvoxamine on the pharmacokinetics of rosiglitazone in healthy subjects. *British Journal of Clinical Pharmacology, 62*, 682–689.

Pei, Q., Liu, J. Y., Yin, J. Y., Yang, G. P., Liu, S. K., Zheng, Y., … Liu, Z. Q. (2018). Repaglinide-irbesartan drug interaction: Effects of SLCO1B1 polymorphism on repaglinide pharmacokinetics and pharmacodynamics in Chinese population. *European Journal of Clinical Pharmacology, 74*, 1021–1028.

Peltoniemi, M. A., Saari, T. I., Hagelberg, N. M., Laine, K., Neuvonen, P. J., & Olkkola, K. T. (2012). St John's wort greatly decreases the plasma concentrations of oral S-ketamine. *Fundamental & Clinical Pharmacology, 26*, 743–750.

Peltoniemi, M. A., Saari, T. I., Hagelberg, N. M., Reponen, P., Turpeinen, M., Laine, K., … Olkkola, K. T. (2011). Exposure to oral S-ketamine is unaffected by itraconazole but greatly increased by ticlopidine. *Clinical Pharmacology and Therapeutics, 90*, 296–302.

Percha, B., & Altman, R. B. (2013). Informatics confronts drug-drug interactions. *Trends in Pharmacological Sciences, 34*, 178–184.

Polepally, A. R., King, J. R., Ding, B., Shuster, D. L., Dumas, E. O., Khatri, A., … Menon, R. M. (2016). Drug–drug interactions between the anti-hepatitis C virus 3D regimen of ombitasvir, paritaprevir/ritonavir, and dasabuvir and eight commonly used medications in healthy volunteers. *Clinical Pharmacokinetics, 55*, 1003–1014.

Qin, W. J., Zhang, W., Liu, Z. Q., Chen, X. P., Tan, Z. R., Hu, D. L., … Zhou, H. H. (2012). Rapid clinical induction of bupropion hydroxylation by metamizole in healthy Chinese men. *British Journal of Clinical Pharmacology, 74*, 999–1004.

Quintieri, L., Palatini, P., Moro, S., & Floreani, M. (2011). Inhibition of cytochrome P450 2C8-mediated drug metabolism by the flavonoid diosmetin. *Drug Metabolism and Pharmacokinetics, 26*, 559–568.

Reyderman, L., Kosoglou, T., Statkevich, P., Pember, L., Boutros, T., Maxwell, S. E., … Batra, V. (2004). Assessment of a multiple-dose drug interaction between ezetimibe, a novel selective cholesterol absorption inhibitor and gemfibrozil. *International Journal of Clinical Pharmacology and Therapeutics, 42*, 512–518.

Robertson, S. M., Maldarelli, F., Natarajan, V., Formentini, E., Alfaro, R. M., & Penzak, S. R. (2008). Efavirenz induces CYP2B6-mediated hydroxylation of bupropion in healthy subjects. *Journal of Acquired Immune Deficiency Syndromes, 49*, 513–519.

Sale, M., & Sherer, E. A. (2015). A genetic algorithm based global search strategy for population pharmacokinetic/pharmacodynamic model selection. *British Journal of Clinical Pharmacology, 79*, 28–39.

Schmid, Y., Rickli, A., Schaffner, A., Duthaler, U., Grouzmann, E., Hysek, C. M., & Liechti, M. E. (2015). Interactions between bupropion and 3,4-methylenedioxymethamphetamine in healthy subjects. *The Journal of Pharmacology and Experimental Therapeutics, 353*, 102–111.

Schmidt, M., & Lipson, H. (2009). Distilling free-form natural laws from experimental data. *Science, 324*, 81–85.

Sinha, V. K., Snoeys, J., Osselaer, N. V., Van Peer, A., Mackie, C., & Heald, D. (2012). From preclinical to human–prediction of oral absorption and drug–drug interaction potential using physiologically based pharmacokinetic (PBPK) modeling approach in an industrial setting: A workflow by using case example. *Biopharmaceutics & Drug Disposition, 33*, 111–121.

Skerjanec, A., Wang, J., Maren, K., & Rojkjaer, L. (2010). Investigation of the pharmacokinetic interactions of deferasirox, a once-daily oral iron chelator, with midazolam, rifampin, and repaglinide in healthy volunteers. *Journal of Clinical Pharmacology, 50*, 205–213.

Soyinka, J. O., Onyeji, C. O., Nathaniel, T. I., Odunfa, O. O., & Ebeshi, B. U. (2013). Effects of concurrent administration of efavirenz on the disposition kinetics of amodiaquine in healthy volunteers. *Journal of Pharmacy Research, 6*, 275–279.

Suttle, A. B., Grossmann, K. F., Ouellet, D., Richards-Peterson, L. E., Aktan, G., Gordon, M. S., … Carson, S. W. (2015). Assessment of the drug interaction potential and single- and repeat-dose pharmacokinetics of the BRAF inhibitor dabrafenib. *Journal of Clinical Pharmacology, 55*, 392–400.

Tabassum, M., & Digital, K. M.-I. J. (2014). *A genetic algorithm analysis towards optimization solutions*. Acad Tabassum, K MathewInternational J Digit Inf Wirel Commun 2014 academia. https://www.academia.edu/download/69674794/A_Genetic_Algorithm_Analysis_towards_Opt20210914-16410-1uwzxjc.pdf.

Tornio, A., Filppula, A. M., Kailari, O., Neuvonen, M., Nyrönen, T. H., Tapaninen, T., … Backman, J. T. (2014). Glucuronidation converts clopidogrel to a strong time-dependent inhibitor of CYP2C8: A phase II metabolite as a perpetrator of drug-drug interactions. *Clinical Pharmacology and Therapeutics, 96*, 498–507.

Tornio, A., Niemi, M., Neuvonen, P. J., & Backman, J. T. (2007). Stereoselective interaction between the CYP2C8 inhibitor gemfibrozil and racemic ibuprofen. *European Journal of Clinical Pharmacology, 63*, 463–469.

Tornio, A., Niemi, M., Neuvonen, P. J., & Backman, J. T. (2008). Trimethoprim and the CYP2C8*3 allele have opposite effects on the pharmacokinetics of pioglitazone. *Drug Metabolism and Disposition, 36*, 73–80.

Turpeinen, M., Tolonen, A., Uusitalo, J., Jalonen, J., Pelkonen, O., & Laine, K. (2005). Effect of clopidogrel and ticlopidine on cytochrome P450 2B6 activity as measured by bupropion hydroxylation. *Clinical Pharmacology and Therapeutics, 77*, 553–559.

Veldkamp, A. I., Harris, M., Montaner, J. S. G., Moyle, G., Gazzard, B., Youle, M., … Hoetelmans, R. M. (2001). The steady-state pharmacokinetics of efavirenz and nevirapine when used in combination in human immunodeficiency virus type 1-infected persons. *The Journal of Infectious Diseases, 184*, 37–42.

Wang, H., & Tompkins, L. (2008). CYP2B6: New insights into a historically overlooked cytochrome P450 isozyme. *Current Drug Metabolism, 9*, 598–610.

Wang, J., Zhang, Z. Y., Lu, S., Powers, D., Kansra, V., & Wang, X. (2019). Effects of rolapitant administered orally on the pharmacokinetics of dextromethorphan (CYP2D6), tolbutamide (CYP2C9), omeprazole (CYP2C19), efavirenz (CYP2B6), and repaglinide (CYP2C8) in healthy subjects. *Support Care Cancer, 27*, 819–827.

Yamazaki, T., Desai, A., Goldwater, R., Han, D., Howieson, C., Akhtar, S., … Townsend, R. (2017). Pharmacokinetic effects of isavuconazole coadministration with the cytochrome P450 enzyme substrates bupropion, repaglinide, caffeine, dextromethorphan, and methadone in healthy subjects. *Clinical Pharmacology in Drug Development, 6*, 54–65.

Yoshida, K., Zhao, P., Zhang, L., Abernethy, D. R., Rekić, D., Reynolds, K. S., … Huang, S. M. (2017). In vitro–in vivo extrapolation of metabolism- and transporter-mediated drug–drug interactions—overview of basic prediction methods. *Journal of Pharmaceutical Sciences, 106*, 2209–2213.

Younis, I. R., Lakota, E. A., Volpe, D. A., Patel, V., Xu, Y., & Sahajwalla, C. G. (2019). Drug-drug interaction studies of methadone and antiviral drugs: Lessons learned. *Journal of Clinical Pharmacology, 59*, 1035–1043.